Life Sciences 232 (2019) 116562

Contents lists available at ScienceDirect

Life Sciences

journal homepage: www.elsevier.com/locate/lifescie

'Stemness' and 'senescence' related escape pathways are dose dependent in lung cancer cells surviving post irradiation

Avgi Tsolou[a], Ioannis Lamprou[a], Alexandra-Ourania Fortosi[a], Maria Liousia[a], Alexandra Giatromanolaki[b], Michael I. Koukourakis[a,*]

[a] Department of Radiotherapy/Oncology, Democritus University of Thrace and University General Hospital of Alexandroupolis, Alexandroupolis 68100, Greece
[b] Department of Pathology, Democritus University of Thrace and University General Hospital of Alexandroupolis, Alexandroupolis 68100, Greece

ARTICLE INFO

Keywords:
Lung cancer
Radiation
DNA-repair
Stemness
Senescence

ABSTRACT

Aims: Lung cancer is one of the main causes of cancer-related deaths worldwide and radiotherapy is a major treatment of choice. However, radioresistance is a main reason for radiotherapy failure or tumor relapse. Here, we investigated possible mechanisms associated with cancer cell radioresistance.

Materials and methods: We compared two newly derived cell lines, namely A549-IR3 and A549-IR6, which survived repeated (3 or 6 times) 4 Gy exposure of parental A549 lung cancer cell line. DNA repair ability, stemness and senescence were comparatively studied.

Key findings: A549-IR3 exhibited higher proliferation ability and radioresistance compared to parental and A549-IR6 cells. Enhanced radioresistance was not accompanied by chemoresistance to cisplatin or docetaxel. DNA repair kinetics (γH2AX expression) were similar in all cell lines. A549-IR3 cells exhibited a significant rise in stem cell markers (CD44, CD133, OCT4, SOX2 and NANOG) whereas A549-IR6 displayed an increased senescent population.

Significance: Cancer cells surviving after radiotherapy may follow two different escape pathways: selection for radioresistance resulting in regrowth, and in clinical terms relapse, or above an irradiation threshold, stem-cells die and cancer cells become senescent, leading the tumor to a state of dormancy.

1. Introduction

Lung cancer is one of the most common fatal malignancies worldwide, accounting for over 1.5 million deaths annually [1]. Non-Small Cell Lung Carcinoma (NSCLC) accounts for 85% of lung cancer cases [2]. Radiotherapy is the treatment of choice for locally advanced inoperable disease [3]. Unfortunately, inherent or acquired radio-resistance counteracts the efficacy radiation therapy, demanding radiotherapy doses impossible to tolerate by neighbouring to cancer normal tissues. The mechanisms defining radio-resistance are complex and include intrinsic pathways like DNA repair capacity [4], metabolic and autophagic activity [5,6] or even microenvironmental factors like hypoxia and immune response [7]. Selection of resistant cancer cell clones during radiotherapy occurs and these become the source of a subsequent tumor relapse [8].

In the current study, we developed two NSCLC cell lines, originating from the A549 cell line. The newly developed cell lines, surviving post multiple radiation, were compared with the parental A549, in terms of relative viability, radioresistance, chemoresistance and repair capacity. Changes in terms of senescence and cancer stem cell population between parental and surviving, after irradiation, cancer cells was also examined.

2. Materials and methods

2.1. Cells lines, culture conditions

A549 non-small cell lung cancer cells [9,10] were purchased from ATCC (ATCC® CCL-185™) and all experiments were performed within 12 months. Details on the cell line can be found at https://www.atcc.org/Products/All/CCL-185.aspx?slp=1#generalinformation.

All cells lines were maintained in Dulbecco's modified Eagle's medium (DMEM) supplemented with 10% FBS, 2 mM L-glutamine, 100 U/ml penicillin and 100 μg/ml streptomycin (Invitrogen), at 37 °C with 5% CO_2 in a humidified incubator. Cell number was determined in duplicates using a haemocytometer.

* Corresponding author at: Department of Radiotherapy/Oncology, Democritus University of Thrace, Alexandroupolis 68100, Greece.
E-mail address: targ@her.forthnet.gr (M.I. Koukourakis).

https://doi.org/10.1016/j.lfs.2019.116562
Received 27 March 2019; Received in revised form 1 June 2019; Accepted 11 June 2019
Available online 12 June 2019

2.2. Development of radioresistant A549 cell lines

Irradiation was performed using a Cobalt-60 Gamma-Ray irradiator (Theratron). A549 lung cancer cell line was subjected to multiple irradiation doses. Firstly, A549 cells were seeded in a 75 cm^2 flask and when they reached ~70% confluence they were irradiated with 4 Gy. Cells were allowed to recover and growth medium was regularly changed every 2 days. Approximately 3 weeks after initial irradiation, and when cells reached a satisfying growth rate (such as parental A549 cells) they were again irradiated with 4 Gy IR. Same procedure was repeated in total 3 times and 6 times to establish the A549-IR3 and the A549-IR6 cell line, respectively.

2.3. Viability/cytotoxicity assays

The viability of A549, A549-IR3 and A549-IR6 was evaluated using the AlamarBlue® Cell Viability Reagent (DAL1100, Invitrogen), as previously described [11]. Radiation dose-response curves were created after exposure of cells to 2, 4, 6 and 8 Gy of radiation and assessing viability on day 8, when the nadir of call counts is noted [11]. Drug treatment included 10 μM cisplatin or 2 nM docetaxel for 24 h and measurement of cell viability 2, 4 and 6 days afterwards. Viability/cytotoxicity experiments were performed in 6-plicates and the mean value was plotted in the figures.

2.4. Assessment of γH2AX kinetics

To follow the repair capacity of each cell line, we examined the levels of γH2AX, a phosphorylated form of histone variant H2AX, which serves as a marker for double-strand breaks (DSBs) [12]. γH2AX expression of nuclear foci was assessed 30 min, 4 h, and 24 h after irradiation with 4 Gy.

Immunofluorescence experiments were performed as previously described [13]. Briefly, paternal A549, A549-IR3, and A549-IR6 cells were grown on coverslips until 50–60% confluence, subjected to the described treatments and fixed in 4% paraformaldehyde. Fixed samples were incubated with anti-γH2AX primary antibody (05-636, Merck, 1:1000) at 4 °C O/N followed by incubation with CF-568 goat anti-mouse IgG (H + L) secondary antibody (1:500, Biotium Cat20100, Lot16C1118) at room temperature, and DNA was counterstained with Hoechst 33342 (1 μg/ml; Sigma-Aldrich). After final washes, coverslips were embedded in a homemade Mowiol 4-88 (cat#81381-250G, Sigma Aldrich, Germany) mounting medium. Imaging was performed on a customized Andor Revolution Spinning Disk Confocal System built around a stand (IX81; Olympus) with a 40× lens and a digital camera (Andor Ixon + 885) (CIBIT Facility, MBG-DUTH). The Andor IQ3 software was used for image acquisition. All confocal microscopy images presented are two-dimensional (2D) maximum intensity projections of z-stack images (ImageJ 1.47v National Institute of Health, USA).

To assess γH2AX kinetics, 8–10 pictures per condition were taken. For each condition, at least 100 cell nuclei were counted in 8–10 randomly chosen fields. Cell nuclei areas were marked and mean fluorescence intensity corresponding to γH2AX foci at the red channel/per nucleus area was calculated, using ImageJ. For the analysis, mean fluorescence value for the total number of cell nuclei examined was calculated.

2.5. Real time-PCR

Real time PCR (RT-PCR) experiments were performed as previously described [14]. Briefly, total RNA was extracted using the Nucleospin RNA Plus kit (740984.50; Macherey-Nagel, Düren, Germany). A reaction mixture suitable for reverse transcription (total volume of 10 μl), containing 500 ng of RNA was prepared for cDNA synthesis with the PrimerScript RT Reagent Kit (RR037A; TaKaRa, Japan). Expression levels of each gene were measured using real-time quantitative PCR (RT-qPCR) and KAPA SYBR FAST qPCR kit (KK4611; KAPA Biosystems, South Africa). The following primer sets with primer sequence 5′→3′ for Forward (L)/Reverse (R) respectively, were designed using the Roche Primer design tool:

CD44: CAACAACACAAATGGCTGGT(L)/CTGAGGTGTCTGTCTCTTTCATCT(R),
CD133: GGAAACTAAGAAGTATGGGAGAACA(L)/CGATGCCACTTTCTCACTGAT(R),
CD24: ATGGGCAGAGCAATGGTG(L)/CCAGTTGTTGTTTCACTGGAAT(R),
ALDH1A1: CCAAAGACATTGATAAAGCCATAA(L)/CACGCCATAGCAATTCACC(R),
C-MYC: GCTGCTTAGACGCTGGATTT(L)/TAACGTTGAGGGGCATCG(R),
NANOG: TCTCCAACATCCTGAACCTCA(L)/TTGCTATTCTTCGGCCAGTT(R),
OCT4: TGAGTAGTCCCTTCGCAAGC(L)/GAGAAGGCGAAATCCGAAG(R),
SOX2: TTGCTGCCTCTTTAAGACTAGGA(L)/TAAGCCTGGGGCTCAAACT(R),
HPRT1: TGACCTTGATTTATTTTGCATACC(L)/CGAGCAAGACGTTCAGTCCT(R).

2.6. Western blotting

For immunoblotting, whole-cell lysates from A549, A549 IR3 and A549 IR6 were used, as previously described in [15]. Lysates were prepared after incubation of cells in ice-cold Lysis Buffer (0.25 M Sucrose, 10 mM Tris pH 7.4) with complete mini protease inhibitor cocktail (Roche Diagnostics, GmbH) and phosphatase inhibitor cocktail (Cell Signalling Technology Inc.) for 30 min, followed by manual scraping and homogenization using a blue pellet pestle. Protein concentrations were determined using the BCA protein assay kit (cat#23225, Pierce, USA) with bovine serum albumin as standard. Samples (20 μg) were analyzed by 10% SDS–PAGE according to standard procedures and transferred onto PVDF membranes. Membranes were probed with primary antibodies against cd44 (ab6124, Abcam) ALDH1A1 (ab52492, Abcam), Oct4 (ab19857, Abcam), cd24 (CM323, Biocare Medical, CA) and cd133 (ab16518, Abcam). Anti-rabbit secondary antibody conjugated with horseradish peroxidase (1:2000; BIORAD) was used and enhanced chemiluminescence was detected using ECL Western blotting substrates (Thermo Fisher Scientific Inc., IL, USA). Equal protein loading was verified by re-probing each membrane with mouse antibody against beta-actin (Nb 600-501; Novus Biologicals).

The blot images were captured utilising a Chemidoc® MP imaging system (Biorad) and band densitometry was analyzed with the accompanying Image Lab software.

2.7. Senescence-associated-β-galactosidase staining

Staining for senescence-associated-β-galactosidase (SA-β-gal) activity was performed as previously described [16]. Briefly, 2×10^5 of untreated A549, A549-IR3 and A549-IR6 cells were seeded on 6-well plates and 24 h later samples were washed with PBS, fixed in 0.2% glutaraldehyde and 2% formaldehyde for 5 min, washed again with PBS, and finally incubated at 37 °C for 24 h in the absence of CO_2, with staining solution (150 mM NaCl, 2 mM $MgCl_2$, 5 mM $K_3[Fe(CN)_6]$, 5 mM $K_4[Fe(CN)_6]$, 40 mM citric acid, and 12 mM sodium phosphate, pH 6.0, containing 1 mg/ml of 5-bromo-4-chloro-3-indolyl-β-d-galactoside (X-gal). Cells showing SA-β-gal staining and the total number of cells were counted in 10 randomly chosen fields per condition.

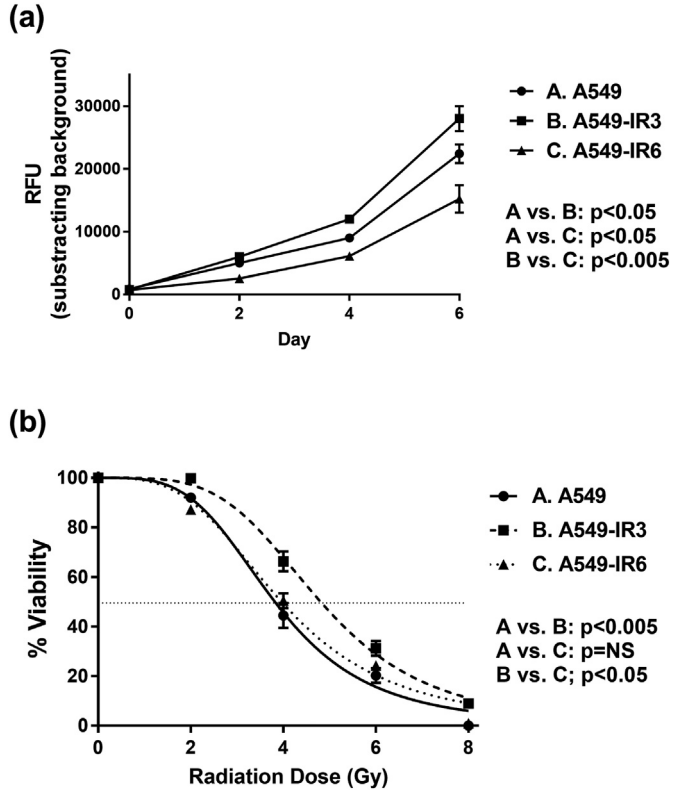

Fig. 1. Survival curves of parental and surviving after irradiation A549 lung cancer cell lines. a) The cell growth rate of untreated A549, A549-IR3, and A549-IR6 during a 6-day time course. b) Cells were acutely irradiated with 2, 4, 6, 8 Gy IR (Day 0), and their viability was measured in the 8th day post-irradiation. Survival of untreated cells is considered as 100%. Experiments were repeated three times, and the graph represents mean survival rates. In both (a) and (b) error bars represent Standard Deviation. Paired and unpaired two-tailed *t*-tests among the 3 different cell lines was performed and relative statistical significance is shown ($p < 0.05$, $p < 0.005$, NS: non significant).

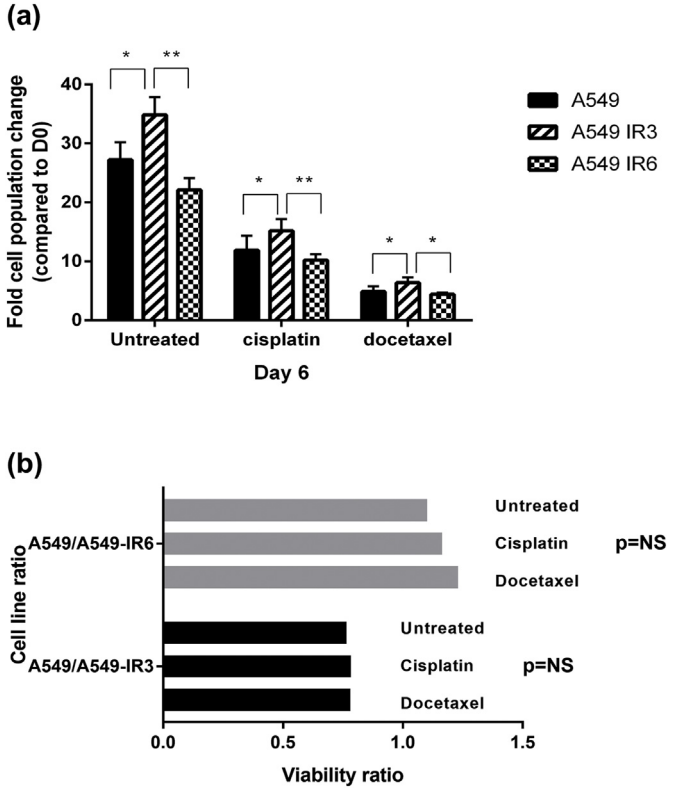

Fig. 2. Survival of parental A549, A549-IR3 and A549-IR6 lung cancer cell lines, post treatment with chemotherapeutic drugs. a) Parental A549, A549-IR3 and A549-IR6 cells were grown without or with cisplatin (10 μM for 24 h) or docetaxel (2 nM for 24 h) and their relative growth rate changes were measured 6 days post-irradiation. The experiment was repeated three times, and graphs represent mean survival rates and Standard Deviation ($^*p < 0.05$, $^{**}p < 0.01$). b) Relative viability ratio of cells treated with chemotherapy vs untreated cells (p = NS).

2.8. Statistical analyses

Statistical analyses and graphical presentation were performed using GraphPad Prism Version 5.01a statistical package (GraphPad Software Inc., USA). Paired and unpaired two-tailed *t*-tests were used for comparisons as appropriate. A *p*-value of < 0.05 was used for determining statistical significance.

3. Results

3.1. Cancer cell proliferation

The proliferation of cancer cells, as measured by the AlamarBlue assay, showed that A549-IR3 cell lines had a significantly higher proliferation rate compared to A549 parental cell line ($p < 0.05$), while the A549-IR6 had a significantly lower growth ability compared to both A549 and A549-IR3 ($p < 0.05$; Fig. 1a).

3.2. Post-irradiation viability

All three cell lines were tested for their relative ability to respond to ionizing radiation (IR). The RD50 (radiation dose required to induce a 50% reduction of cell viability) was 3.8 Gy for A549, 4.8 Gy for A549-IR3 and 3.9 Gy for A549-IR6 (Fig. 1b). The A549-IR3 had a significantly higher post-irradiation viability compared to A549 and A549-IR6 ($p < 0.05$).

3.3. Post-chemotherapy viability

Next, we investigated whether A549 cells surviving after multiple irradiations have different sensitivity to chemotherapeutic drugs. Cells were treated with either cisplatin 10 μM or docetaxel 2 nM for 24 h, and cell viability was monitored 2, 4 and 6 days later. A549-IR3 cells sustained its higher proliferation rate compared to A549 and A549-IR6, under exposure to drugs (Fig. 2a). Similarly, A549-IR6 cell line maintained a lower proliferation activity under exposure to cisplatin or docetaxel (Fig. 2a). Analyzing the ratio of viability, chemosensitivity was not different among the A549 parental and surviving after irradiation IR3 and IR6 cell lines (Fig. 2b).

3.4. γH2Ax assessed DNA double-strand break repair kinetics

Parental A549, and A549-IR3 and A549-IR6 cell lines were irradiated with 4 Gy, and their ability to repair DNA damage was determined by γH2AX. Immunofluorescent confocal analysis showed that in all cases, cells retain their ability to respond to genotoxic stress since γH2AX foci increase in the nuclei as early as 30 min post IR (Fig. 3A). The number of the γH2AX foci induced by radiation was not significantly different among cell lines. The kinetics of γH2AX foci was assessed at 4 h and 24 h post-irradiation, showing a similar rate of regression in all three cell lines (Fig. 3B).

3.5. Stem cell marker analysis

Next, we sought to investigate the cancer stem cell population in the

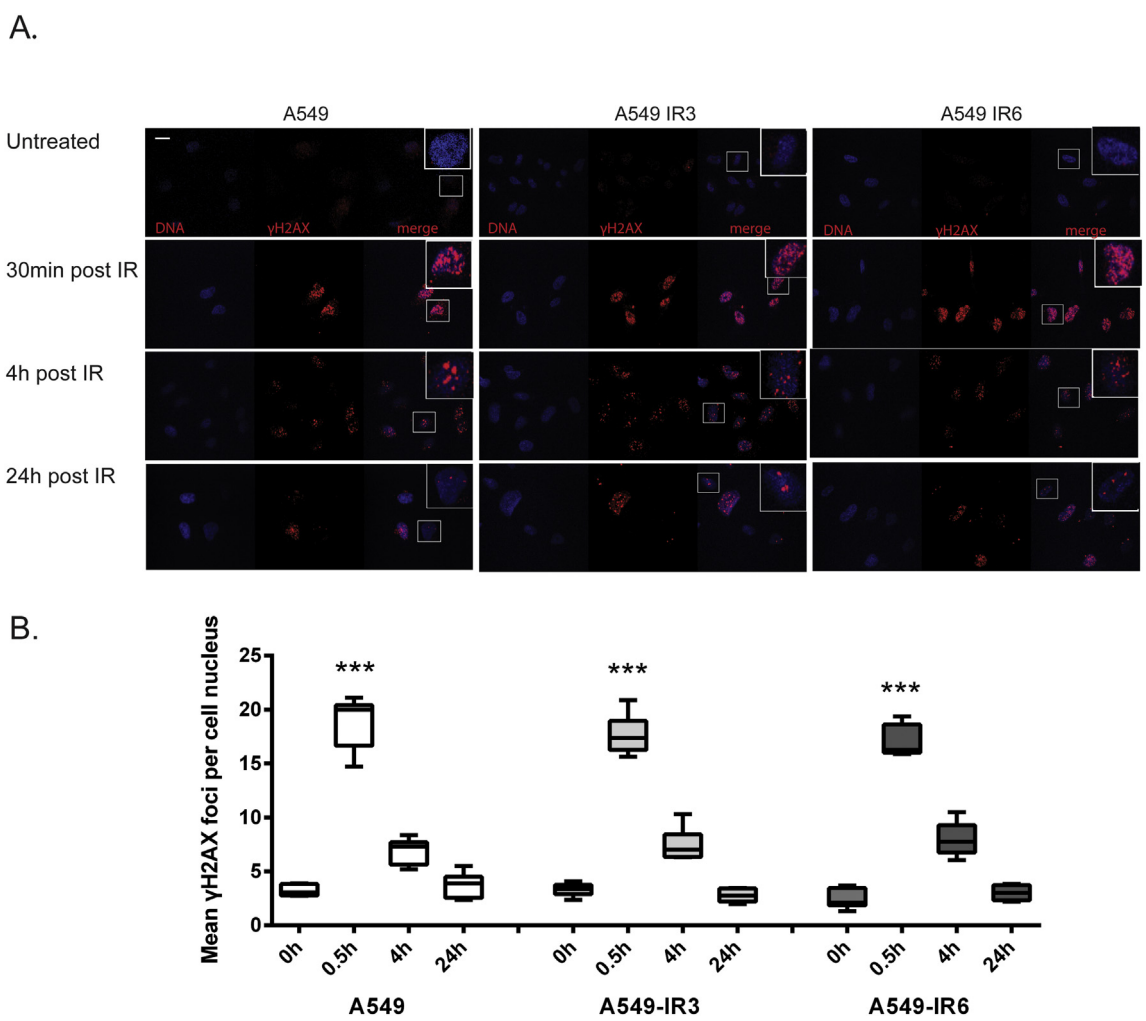

Fig. 3. γH2AX post-irradiation kinetics in three NSCLC lung cancer cell lines. A) Representative images of γH2AX stained A549, A549-IR3 and A549-IR6 cells at the indicated time-points, following 4 Gy irradiation. Inset pictures show a magnified image of the highlighted cell. Hoechst 33342 was used as the nuclear marker. Scale bar denotes 10 nm. B) Quantification of the mean fluorescence intensity of γH2AX per nucleus after irradiation at the indicated time points from three independent experiments. Data show mean ± SD.

three cell lines. Thus, mRNA levels of various stem cell markers were measured in A549, A549-IR3, and A549-IR6 cells. RT-PCR analysis demonstrated that mRNA levels of CD44 were strongly induced in A549-IR3 cells ($2^{-\Delta\Delta Ct}$ 15.9 fold, compared to A549), while they returned to almost basal levels in A549-IR6 (1.7 fold compared to A549; $p < 0.001$). In contrast, CD24 mRNA levels remained unaltered in IR3 and IR6 cell lines (p = NS). CD133, OCT4, SOX2, and NANOG mRNA levels were also strongly induced in A549-IR3 cells ($p < 0.001$). CD133 and ALDH1A1 were significantly increased in the A549-IR6 cell line ($p < 0.001$ and $p < 0.05$, respectively) (Fig. 4A). Additionally, protein expression analysis of stem cell markers in all three cell lines tested, fortified the aforementioned findings (Fig. 4B).

3.6. Senescence analysis

We then tested senescence-associated beta-galactosidase (sen-beta-gal) activity, a known biochemical marker of cellular senescence [16], in A549, A549-IR3, and A549-IR6 cells. Non-irradiated cells from all three cell lines were fixed and stained for sen-beta-gal, and the percentage of cells stained blue was calculated in the total number of cells counted. In parental A549 cells, the percentage of positive β-galactosidase-stained senescent cells was 1.2% ± 0.8%. A small, still significant increase in this percentage was noted in A549-IR3 cells (6.4% ± 2%, $p < 0.05$). A robust significant increase was observed in the A549-IR6 cell line (14.4% ± 3.8%, $p < 0.001$) (Fig. 4C–D).

4. Discussion

Radiotherapy is a leading treatment for locally advanced NSCLC. Investigating the changes in the biology of cells that persist after irradiation is essential to understand the nature of clinical radioresistance, and may help to identify interventions that would improve the efficacy of radiotherapy. With the current work, we aimed to clarify possible factors that may be activated in cells surviving after irradiation and may account for clinical radioresistance and local tumor relapse. To this end, two new NSCLC cell lines, namely A549-IR3 and A549-IR6 were developed, from cells surviving after 3 and six irradiations with 4 Gy (3 weeks apart) of parental A549 cells, respectively.

First, we demonstrated that A549-IR3 cells, exposed to mild levels of radiation (3 fractions of 4 Gy, 3-weeks apart) exhibit an intensified proliferation ability and increased viability following escalated doses of radiotherapy. This is important, as mild radiotherapy doses seem to allow the development of cancer cell clones with increased resistance to radiation. On the contrary, heavily irradiated surviving A549-IR6 cells (6 fractions of 4 Gy, three weeks apart) had a growth activity similar to the parental cells and were more vulnerable to escalated doses of radiotherapy. Thus, heavily irradiated tumors become repopulated by cancer cells suffering a high burden of radiation-induced damage, so

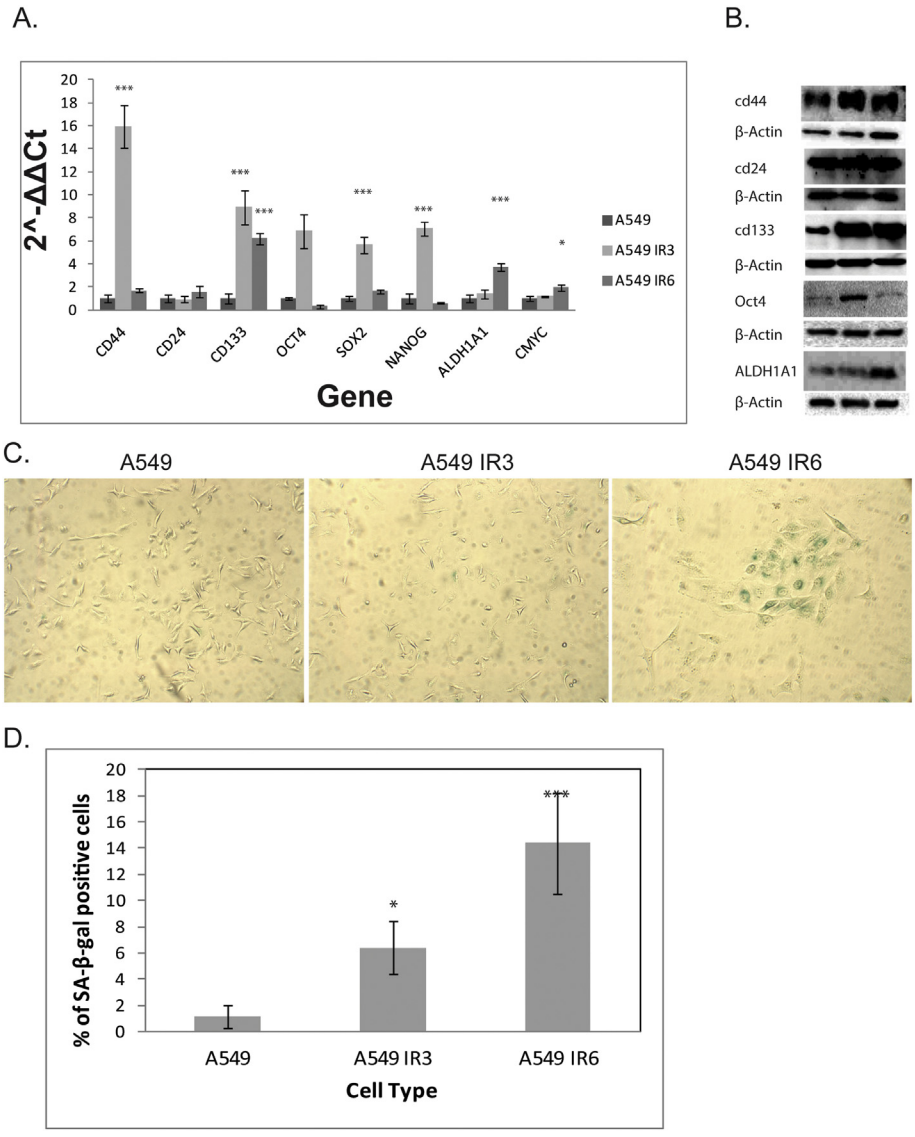

Fig. 4. Expression of stem cell and senescent markers in A549-IR3, A549-IR6 cells, and their parental A549 cell line. A) Relative quantitative analysis of mRNA levels of CD44, CD24, CD133, Oct4, Sox2, NANOG, ALDH1A1 and c-Myc mRNA levels in three NSCLC cell lines. Statistical significance is denoted with asterisks, $*p < 0.05$, $***p < 0.001$. B) Immunoblot analysis demonstrating relative protein expression of Cd44, Cd24, Cd133, Oct4 and ALDH1A1 in A549, A549-IR3, A549-IR6 cells. B-actin was used as a loading control for each immunoblot. C) Sen-β-gal staining in A549, A549-IR3, and A549-IR6 cells. Representative images of A549, A549-IR3, and A549-IR6 cells, taken with 20× objective. D) Graph demonstrating percentage (%) of SA-β-gal positive cells in 3 cell populations. Data show mean ± SD from three independent experiments. Statistical significance is denoted with asterisks, $*p < 0.05$, $***p < 0.001$.

that cumulative lethal radiation damage occurs after further irradiation. This finding could have a clinical significance, as after radical high dose radiotherapy of lung cancer, remnant cancer cells may be more sensitive to additional radiation. Mild escalation of the radiotherapy dose may, thus, be crucial to achieving complete tumor eradication. Indeed, clinical trials support the escalation of the dose of radiotherapy, although fatal pneumonitis is a limiting toxicity [17,18].

Another way to extrapolate the above findings in the clinical practice is to add DNA-repair inhibitors during radiotherapy [19]. This is a well-documented hypothesis by randomized clinical trials showing improved radiotherapy efficacy by combing radiation with cisplatin, a DNA intercalation agent [20,21]. It was anticipated that cancer cells surviving after radiotherapy would become gradually more vulnerable to radiation and chemotherapy, by reducing their capacity to repair DNA damage. In contrast, however, to what expected, the induction of DNA-DSBs (DNA double-strand breaks) and their repair kinetics were identical in parental, mildly irradiated and heavily irradiated surviving cancer cells. As parental and irradiated cells remain DNA-repair efficient, DNA damage seems not the main, or at least the only, pathway to target to eradicate remnant irradiated lung cancer cells. Of interest, all three cell lines were equally sensitive to cisplatin and docetaxel, suggesting that radiotherapy does not sensitize cancer cells to further chemotherapy. Thus, as DNA-repair independent biological pathways may account for the survival of cancer cells after mild or heavy irradiation, post-radiotherapy chemotherapy with conventional drugs seems not to be a therapeutic means to specifically target such cells.

Mild irradiation of parental lung cancer produced an aggressive cell line, with high proliferation ability and more resistant to further irradiation, which although had similar DNA repair abilities with the parental cell line, was composed by a cell population expressing various cancer stem-cell markers, like CD44, CD133, OCT4, SOX, NANOG and stable levels of CD24. This finding is in full accordance with a previous study by Gomez-Casal et al. [22]. CD44 + /CD24 − cells are considered markers of stem cells in a variety of solid tumors [23–25]. Expression of CD44 and Oct4 were significantly associated with the MIB-1 proliferation index and with poor prognosis of patients with head-neck squamous cancer undergoing radiotherapy [26]. Several in vitro studies have shown that CD44 overexpression defines radioresistance of various types of cancer cells [27–29]. Numerous experimental studies also support the involvement of other stem-cell markers like Oct4, Sox2 or NANOG in resistance to radiation [30,31]. It seems, therefore, that repopulation of tumors by radioresistant stem-cells after mild levels of irradiation is a principal pathway defining tumor persistence and regrowth.

Therapeutic approaches that target such cancer stem-cells may be essential for tumor eradication. Humanized monoclonal anti-CD44

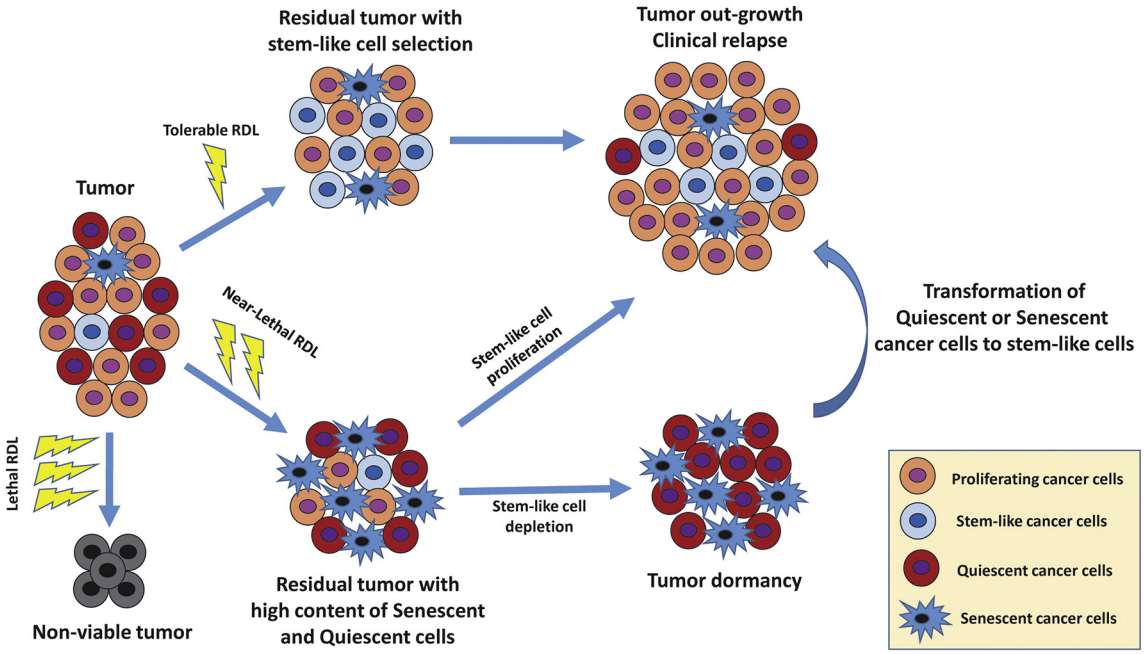

Fig. 5. Schematic representation of possible alternative pathways followed by tumor cells, upon differential tolerance of irradiation. RDL stands for radiation dose level.

antibodies and pharmacological inhibitors of CD44 have been developed and tested in phase I/II trials [32]. SOX2, for instance, has been used as a target for cancer immunotherapy, as peptides from its protein stimulate anti-cancer immune response [33]. Several compounds have also shown a specific activity on SOX2-expressing cancer cells [34,35]. CD133 is also under intense investigation as a target for therapy [36]. Targeting cancer stem-cells would, therefore, be necessary for increasing the eradication of tumors, with even lower doses of radiotherapy, which would, in turn, decrease side-effects from ultra-high radiotherapy doses required in radio-resistant tumors.

Another interesting finding was that lung cancer cells surviving after high doses of radiotherapy are no longer highly populated by cancer stem-cells as noted after mild radiotherapy doses. Such cells, however, overexpressed ALDHA1. This marker is quite contradictory as, although it is considered a stem-cell marker, low levels of ALDHA1 may also characterize cancer cells with stem-cell activity [37]. What, however, was impressively increased in heavily irradiated surviving cancer cells, was the percentage of cancer cells that had entered senescence. The induction of cellular senescence by ionizing radiation is supported by numerous studies. Sub-cytotoxic doses of radiation have been shown to induce replicative senescence that often involves telomere instability [38]. Activation of the ATM-p52-p21 pathway by radiation-induced DNA double strand breaks is an important step for G1-phase arrest. Irreparable DNA damage leads cells to trigger premature senescence pathways by activating p16 expression [39]. In the current study, we confirm the induction of senescence in a high percentage of heavily irradiated A549 cancer cells (A549-IR6), which are also characterized by reduced proliferation rate and lack of expression of stem cell markers. This state simulates radiation induce dormancy often met in the clinical practice, where after obtaining tumor shrinkage a remnant mass persists for long periods before it starts again to progress [40]. An interesting recent study suggests that cancer cells that entered senescence after chemotherapy may be released from senescence and re-enter the cell cycle with higher Wnt-dependent clonogenic growth compared to cancer cells that had never been exposed to chemotherapy [41]. It seems, therefore, that to increase the efficacy of the maximum tolerable dose of radiotherapy, especially in cases with clinically documented tumor dormancy, senescent cells may be an essential target [42].

5. Conclusions

According to irradiation 'heaviness', cancer cells surviving post IR may follow two main types of survival response. Tolerable irradiation doses may "select" for radioresistant cancer stem-cells. Despite the tumor shrinkage induced by the radiotherapy-mediated depopulation, such cells will start to re-grow leading to local relapse. This is the '*stemness sustained escape pathway*.' Prevalence of this pathway, however, is allowed up to a certain radiation dose level, as above this stem-cells are gradually depleted due to over-irradiation. At these near-eradication radiation dose levels, cancer cells may follow the senescence/quiescence pathway, leading the tumor to a state of dormancy, which can be established at a subclinical (complete radiological response) or clinical (evident remnant tumor mass) level. Such cells may re-program their biology months or years after irradiation, by re-activating stemness, and producing tumors with enhanced growth and metastatic ability. This is the '*senescence sustained escape pathway*' (Fig. 5).

Funding

This work was supported by the Democritus University of Thrace Special Account, Project No 81006.

Declaration of Competing Interest

The authors declare that there are no conflicts of interest.

Acknowledgements

We thank Dr Glyn Nelson for his useful comments on the manuscript.

References

[1] L.A. Torre, F. Bray, R.L. Siegel, J. Ferlay, J. Lortet-Tieulent, A. Jemal, Global cancer statistics, 2012, CA Cancer J. Clin. 65 (2015) 87–108.
[2] J.R. Molina, P. Yang, S.D. Cassivi, S.E. Schild, A.A. Adjei, Non-small cell lung cancer: epidemiology, risk factors, treatment, and survivorship, Mayo Clin. Proc. 83 (2008) 584–594.
[3] W.E. Eberhardt, D. De Ruysscher, W. Weder, C. Le Pechoux, P. De Leyn,

H. Hoffmann, V. Westeel, R. Stahel, E. Felip, S. Peters, 2nd ESMO Consensus Conference in Lung Cancer: locally advanced stage III non-small-cell lung cancer, Ann. Oncol. 26 (2015) 1573–1588.
[4] E.H. Stover, P.A. Konstantinopoulos, U.A. Matulonis, E.M. Swisher, Biomarkers of response and resistance to DNA repair targeted therapies, Clin. Cancer Res. 22 (2016) 5651–5660.
[5] L. Tang, F. Wei, Y. Wu, Y. He, L. Shi, F. Xiong, Z. Gong, C. Guo, X. Li, H. Deng, K. Cao, M. Zhou, B. Xiang, Y. Li, G. Li, W. Xiong, Z. Zeng, Role of metabolism in cancer cell radioresistance and radiosensitization methods, J. Exp. Clin. Cancer Res. 37 (2018) 87.
[6] K.-C. Chow, A cytological link between radioresistance and autophagy, Transl. Cancer Res. (2016) S1354–S1357.
[7] Y. Sun, Tumor microenvironment and cancer therapy resistance, Cancer Lett. 380 (2016) 205–215.
[8] K. Rycaj, D.G. Tang, Cancer stem cells and radioresistance, Int. J. Radiat. Biol. 90 (2014) 615–621.
[9] J.U. Balis, S.D. Bumgarner, J.E. Paciga, J.F. Paterson, S.A. Shelley, Synthesis of lung surfactant-associated glycoproteins by A549 cells: description of an in vitro model for human type II cell dysfunction, Exp. Lung Res. 6 (1984) 197–213.
[10] S. Yusein-Myashkova, I. Stoykov, A. Gospodinov, I. Ugrinova, E. Pasheva, The repair capacity of lung cancer cell lines A549 and H1299 depends on HMGB1 expression level and the p53 status, J. Biochem. 160 (2016) 37–47.
[11] M.A. Zachari, P.S. Chondrou, S.E. Pouliliou, A.G. Mitrakas, I. Abatzoglou, C.E. Zois, M.I. Koukourakis, Evaluation of the alamarblue assay for adherent cell irradiation experiments, Dose-Response 12 (2014) 246–258.
[12] T.T. Paull, E.P. Rogakou, V. Yamazaki, C.U. Kirchgessner, M. Gellert, W.M. Bonner, A critical role for histone H2AX in recruitment of repair factors to nuclear foci after DNA damage, Curr. Biol. 10 (2000) 886–895.
[13] A. Tsolou, G. Nelson, V. Trachana, N. Chondrogianni, G. Saretzki, T. von Zglinicki, E.S. Gonos, The 19S proteasome subunit Rpn7 stabilizes DNA damage foci upon genotoxic insult, IUBMB Life 64 (2012) 432–442.
[14] A. Giatromanolaki, M. Liousia, S. Arelaki, D. Kalamida, S. Pouliliou, A. Mitrakas, A. Tsolou, E. Sivridis, M.I. Koukourakis, Differential effect of hypoxia and acidity on lung cancer cell and fibroblast metabolism, Biochem. Cell Biol. 95 (2017) 428–436.
[15] A. Tsolou, M. Liousia, D. Kalamida, S. Pouliliou, A. Giatromanolaki, M. Koukourakis, Inhibition of IKK-NFkappaB pathway sensitizes lung cancer cell lines to radiation, Cancer Biol. Med. 14 (2017) 293–301.
[16] G.P. Dimri, X. Lee, G. Basile, M. Acosta, G. Scott, C. Roskelley, E.E. Medrano, M. Linskens, I. Rubelj, O. Pereira-Smith, et al., A biomarker that identifies senescent human cells in culture and in aging skin in vivo, Proc. Natl. Acad. Sci. U. S. A. 92 (1995) 9363–9367.
[17] J. Ramroth, D.J. Cutter, S.C. Darby, G.S. Higgins, P. McGale, M. Partridge, C.W. Taylor, Dose and fractionation in radiation therapy of curative intent for non-small cell lung cancer: meta-analysis of randomized trials, Int. J. Radiat. Oncol. Biol. Phys. 96 (2016) 736–747.
[18] P.G. Tsoutsou, M.I. Koukourakis, Radiation pneumonitis and fibrosis: mechanisms underlying its pathogenesis and implications for future research, Int. J. Radiat. Oncol. Biol. Phys. 66 (2006) 1281–1293.
[19] M. O'Driscoll, P.A. Jeggo, The role of double-strand break repair - insights from human genetics, Nat. Rev. Genet. 7 (2006) 45–54.
[20] M.I. Koukourakis, P.G. Tsoutsou, A. Karpouzis, M. Tsiarkatsi, I. Karapantzos, V. Daniilidis, C. Kouskoukis, Radiochemotherapy with cetuximab, cisplatin, and amifostine for locally advanced head and neck cancer: a feasibility study, Int. J. Radiat. Oncol. Biol. Phys. 77 (2010) 9–15.
[21] M. Wei, Q. Ye, X. Wang, M. Wang, Y. Hu, Y. Yang, J. Yang, J. Cai, Early tumor shrinkage served as a prognostic factor for patients with stage III non-small cell lung cancer treated with concurrent chemoradiotherapy, Medicine (Baltimore) 97 (2018) e0632.
[22] R. Gomez-Casal, C. Bhattacharya, N. Ganesh, L. Bailey, P. Basse, M. Gibson, M. Epperly, V. Levina, Non-small cell lung cancer cells survived ionizing radiation treatment display cancer stem cell and epithelial-mesenchymal transition phenotypes, Mol. Cancer 12 (2013) 94.
[23] A. Jaggupilli, E. Elkord, Significance of CD44 and CD24 as cancer stem cell markers: an enduring ambiguity, Clin. Dev. Immunol. 2012 (2012) 708036.
[24] M.G. Slomiany, L. Dai, L.B. Tolliver, G.D. Grass, Y. Zeng, B.P. Toole, Inhibition of functional hyaluronan-CD44 interactions in CD133-positive primary human ovarian carcinoma cells by small hyaluronan oligosaccharides, Clin. Cancer Res. 15 (2009) 7593–7601.
[25] H.J. Lee, G. Choe, S. Jheon, S.W. Sung, C.T. Lee, J.H. Chung, CD24, a novel cancer biomarker, predicting disease-free survival of non-small cell lung carcinomas: a retrospective study of prognostic factor analysis from the viewpoint of forthcoming (seventh) new TNM classification, J. Thorac. Oncol. 5 (2010) 649–657.
[26] M.I. Koukourakis, A. Giatromanolaki, V. Tsakmaki, V. Danielidis, E. Sivridis, Cancer stem cell phenotype relates to radio-chemotherapy outcome in locally advanced squamous cell head-neck cancer, Br. J. Cancer 106 (2012) 846–853.
[27] K. Tsubouchi, K. Minami, N. Hayashi, Y. Yokoyama, S. Mori, H. Yamamoto, M. Koizumi, The CD44 standard isoform contributes to radioresistance of pancreatic cancer cells, J. Radiat. Res. 58 (2017) 816–826.
[28] C.T. Wu, W.Y. Lin, Y.H. Chang, W.C. Chen, M.F. Chen, Impact of CD44 expression on radiation response for bladder cancer, J. Cancer 8 (2017) 1137–1144.
[29] J. Ni, P.J. Cozzi, J.L. Hao, J. Beretov, L. Chang, W. Duan, S. Shigdar, W.J. Delprado, P.H. Graham, J. Bucci, J.H. Kearsley, Y. Li, CD44 variant 6 is associated with prostate cancer metastasis and chemo-/radioresistance, Prostate 74 (2014) 602–617.
[30] S. Ventela, E. Sittig, L. Mannermaa, J.A. Makela, J. Kulmala, E. Loyttyniemi, L. Strauss, O. Carpen, J. Toppari, R. Grenman, J. Westermarck, CIP2A is an Oct4 target gene involved in head and neck squamous cell cancer oncogenicity and radioresistance, Oncotarget 6 (2015) 144–158.
[31] L. Shen, X. Huang, X. Xie, J. Su, J. Yuan, X. Chen, High expression of SOX2 and OCT4 indicates radiation resistance and an independent negative prognosis in cervical squamous cell carcinoma, J. Histochem. Cytochem. 62 (2014) 499–509.
[32] C. Chen, S. Zhao, A. Karnad, J.W. Freeman, The biology and role of CD44 in cancer progression: therapeutic implications, J. Hematol. Oncol. 11 (2018) 64.
[33] R. Favaro, I. Appolloni, S. Pellegatta, A.B. Sanga, P. Pagella, E. Gambini, F. Pisati, S. Ottolenghi, M. Foti, G. Finocchiaro, P. Malatesta, S.K. Nicolis, Sox2 is required to maintain cancer stem cells in a mouse model of high-grade oligodendroglioma, Cancer Res. 74 (2014) 1833–1844.
[34] X. Zhang, F. Lu, J. Wang, F. Yin, Z. Xu, D. Qi, X. Wu, Y. Cao, W. Liang, Y. Liu, H. Sun, T. Ye, H. Zhang, Pluripotent stem cell protein Sox2 confers sensitivity to LSD1 inhibition in cancer cells, Cell Rep. 5 (2013) 445–457.
[35] E. Yokota, T. Yamatsuji, M. Takaoka, M. Haisa, N. Takigawa, N. Miyake, T. Ikeda, T. Mori, S. Ohno, T. Sera, T. Fukazawa, Y. Naomoto, Targeted silencing of SOX2 by an artificial transcription factor showed antitumor effect in lung and esophageal squamous cell carcinoma, Oncotarget 8 (2017) 103063–103076.
[36] P.M. Glumac, C.L. Forster, H. Zhou, P. Murugan, S. Gupta, A.M. LeBeau, The identification of a novel antibody for CD133 using human antibody phage display, Prostate 78 (2018) 981–991.
[37] K. Okudela, T. Woo, H. Mitsui, T. Suzuki, M. Tajiri, Y. Sakuma, Y. Miyagi, Y. Tateishi, S. Umeda, M. Masuda, K. Ohashi, Downregulation of ALDH1A1 expression in non-small cell lung carcinomas—its clinicopathologic and biological significance, Int. J. Clin. Exp. Pathol. 6 (2013) 1–12.
[38] S.A. Stewart, I. Ben-Porath, V.J. Carey, B.F. O'Connor, W.C. Hahn, R.A. Weinberg, Erosion of the telomeric single-strand overhang at replicative senescence, Nat. Genet. 33 (2003) 492–496.
[39] K. Suzuki, I. Mori, Y. Nakayama, M. Miyakoda, S. Kodama, M. Watanabe, Radiation-induced senescence-like growth arrest requires TP53 function but not telomere shortening, Radiat. Res. 155 (2001) 248–253.
[40] A.S. Yadav, P.R. Pandey, R. Butti, N.N.V. Radharani, S. Roy, S.R. Bhalara, M. Gorain, G.C. Kundu, D. Kumar, The biology and therapeutic implications of tumor dormancy and reactivation, Front. Oncol. 8 (2018) 72.
[41] M. Milanovic, D.N.Y. Fan, D. Belenki, J.H.M. Dabritz, Z. Zhao, Y. Yu, J.R. Dorr, L. Dimitrova, D. Lenze, I.A. Monteiro Barbosa, M.A. Mendoza-Parra, T. Kanashova, M. Metzner, K. Pardon, M. Reimann, A. Trumpp, B. Dorken, J. Zuber, H. Gronemeyer, M. Hummel, G. Dittmar, S. Lee, C.A. Schmitt, Senescence-associated reprogramming promotes cancer stemness, Nature 553 (2018) 96–100.
[42] V. Myrianthopoulos, K. Evangelou, P.V.S. Vasileiou, T. Cooks, T.P. Vassilakopoulos, G.A. Pangalis, M. Kouloukoussa, C. Kittas, A.G. Georgakilas, V.G. Gorgoulis, Senescence and senotherapeutics: a new field in cancer therapy, Pharmacol. Ther. 193 (2019) 31–49.